

Imaging of dentate nucleus pathologies; a pictorial essay

Kajari Bhattacharya, Hima Pendharkar, Arun K Gupta

Department of Neuroimaging and Interventional Radiology, NIMHANS, Bengaluru, Karnataka, India

Correspondence: Dr. Hima Pendharkar, Department of Neuroimaging and Interventional Radiology, NIMHANS, Hosur Road, Bengaluru, Karnataka - 560 029, India. E-mail: himasp1@gmail.com

Abstract

Dentate nucleus is affected in a wide variety of conditions. Magnetic resonance imaging of the brain is the diagnostic modality of choice for delineating the signal characteristics, which helps in narrowing down a vast list of differentials for conditions affecting the dentate. Computed tomography plays an important role, especially for pathologies associated with calcification of dentate nucleus. The purpose of this essay is to demonstrate the host of conditions associated with imaging abnormalities in dentate nuclei in patients with varied clinical features.

Key words: CT; dentate nucleus; magnetic resonance imaging

Introduction

Dentate nucleus is the largest of deep cerebellar nuclei. It has a predictable imaging appearance with respect to the surrounding cerebellar white matter during the first year of life. At term it is hypointense on T1 and hyperintense with a dark serrated rim on T2. By 6 months of age, it remains slightly brighter on T2-weighted (T2W) images and the hypointense rim cannot be separately distinguished from the surrounding cerebellar white matter.^[1] Therefore, increased signal in dentate nucleus on T2W or fluid-attenuated inversion recovery (FLAIR) sequences beyond 6 months is abnormal. Diffusion restriction at any age is abnormal.^[2]

Numerous conditions can affect the dentate nuclei. A recent review^[3] elucidated the clinico-radiological approach to aid the diagnosis and management of these conditions. Careful assessment of the differential involvement of dentate hilus, peridentate white matter, rest of the cerebellar white matter,

cerebellar gray matter and brainstem, and supratentorial abnormalities can help narrow down the possibilities.

We present a pictorial review of the various pathologies affecting dentate nuclei and their imaging findings encountered in our institute.

Role of computed tomography

The role of computed tomography (CT) is well established in identifying the variety of conditions known to cause calcifications in the dentate nuclei [Table 1].^[4] If present, it narrows down the differential diagnosis in accordance with the age at presentation, history, and clinical features.

Role of magnetic resonance imaging

For eliciting the subtle signal changes in the dentate with associated abnormalities of the rest of the brain and spinal cord, magnetic resonance imaging (MRI) is the investigation of choice. Sequences which are routinely acquired include T1, T2, susceptibility-weighted imaging (SWI)/gradient

This is an open access journal, and articles are distributed under the terms of the Creative Commons Attribution-NonCommercial-ShareAlike 4.0 License, which allows others to remix, tweak, and build upon the work non-commercially, as long as appropriate credit is given and the new creations are licensed under the identical terms.

For reprints contact: reprints@medknow.com

Cite this article as: Bhattacharya K, Pendharkar H, Gupta AK. Imaging of dentate nucleus pathologies; a pictorial essay. Indian J Radiol Imaging 2018;28:152-60.

Access this article online

Quick Response Code:



Website:
www.ijri.org

DOI:
10.4103/ijri.IJRI_290_17

Table 1: Causes of dentate nucleus calcification

Physiological
Age related
Congenital/hereditary disorders
Cockayne syndrome
Primary familial brain calcification/Fahr's syndrome
Aicardi-Goutiere's syndrome
Leukoencephalopathy with calcifications and cysts (LCC)
MELAS
Spinocerebellar ataxia type-20
Cerebrotendinous xanthomatosis
Endocrine
Hypothyroidism
Hypoparathyroidism
Hyperparathyroidism
Pseudohypoparathyroidism
Post-thyroidectomy
Others
Lead poisoning
Lupus erythematosus
Hypoxic ischemic encephalopathy

echo (GRE), diffusion-weighted imaging (DWI) and postcontrast T1W imaging.

Conditions affecting dentate nuclei and their imaging appearance

These conditions have been elaborately described by Van der Knaap^[5].

Leukodystrophies

Krabbe's disease or globoid cell leukodystrophy is an autosomal recessive disorder caused by the deficiency of galactocerebroside β -galactosidase causing accumulation of cerebroside in lysosomes of white matter forming characteristic globoid cells. Subtypes include early infantile (most common), late infantile onset, juvenile, and adolescent. CT plays an important role as bilateral hyperdense thalami are a characteristic feature of this entity. MRI shows T2/FLAIR hyperintensity in the periventricular white matter and occasionally optic nerve/chiasma hypertrophy. Dentate may be involved. Postcontrast images may show nerve enhancement [Figure 1].

Alexander's disease is a nonfamilial leukoencephalopathy presenting in, infantile, juvenile, or adult forms. Most reported cases are infantile onset presenting with global developmental delay. Characteristic MRI findings include extensive supratentorial white matter hyperintensities with frontal predominance and involvement of subcortical white matter. Signal changes are also noted in the basal ganglia. T1 hyperintense, T2 hypointense capping is noted adjacent to the frontal horns bilaterally. Postcontrast images reveal enhancement of the periventricular rim and the dentate nucleus [Figure 2].

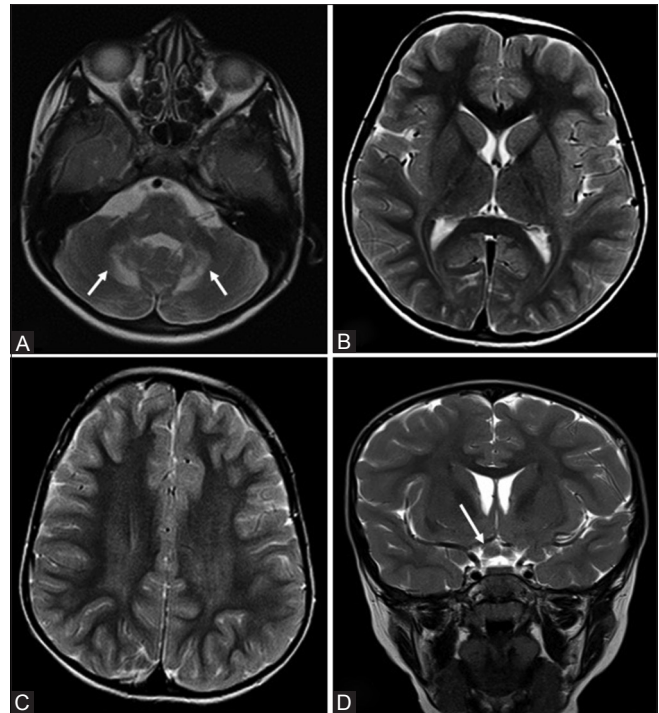


Figure 1 (A-D): Krabbe's disease – A 2-year-old girl presented with hyperirritability, hypertonia, fever, and developmental regression with cognitive decline and nystagmus for the past 6 months. CT (not shown) showed bilateral hyperdense thalami. (A) Axial T2WI shows symmetrical hyperintensity in bilateral dentate nuclei (*white arrows*), (B) with subtle signal changes in the posterior limb of internal capsules and (C) corona radiata. (D) Coronal T2WI shows hypertrophy of the right half of optic chiasma (*white arrow*). No postcontrast enhancement was noted in this case (not shown)

Canavan's disease or spongiform leukodystrophy is an autosomal recessive disorder caused by the deficiency of N-acetylaspartylase (NAA). The condition is characterized by early onset macrocephaly. MRI shows diffuse T2/FLAIR hyperintensity in the supratentorial white matter. Globus pallidus is involved. Magnetic resonance spectroscopy (MRS) shows a large NAA peak [Figure 3].

Aicardi-Goutiere's syndrome is an autosomal recessive disorder characterized by microcephaly, chronic cerebrospinal fluid (CSF) lymphocytosis, and raised levels of CSF interferon- α . Onset is typically in the first year of life with feeding difficulties, low-grade fever, progressive truncal hypotonia, severe pyramidal and extrapyramidal signs, and skin lesions. MRI may show diffuse white matter hyperintensity in T2/FLAIR with punctate calcifications. Cystic change is known in this entity [Figure 4].

Metabolic, toxin, and drug-induced

Maple syrup urine disease shows enzymatic defect in the initial steps of the common metabolic pathway for breakdown of branched-chain amino acids – leucine, isoleucine, and valine – leading to the accumulation of corresponding keto acids. Infants generally present with failure to thrive. CT shows a very characteristic pattern

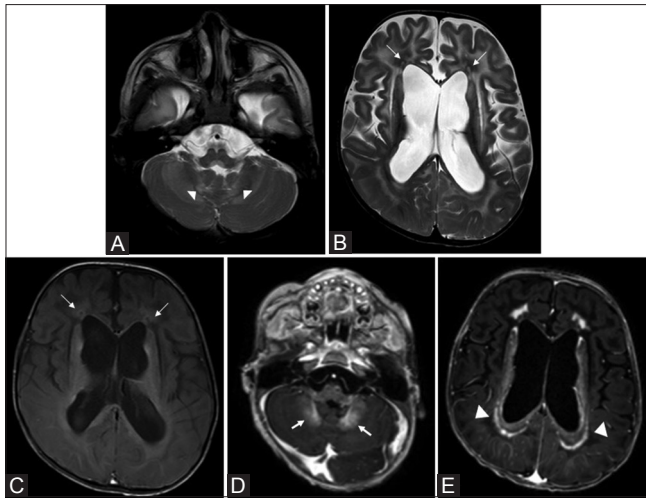


Figure 2 (A-E): Alexander's disease – A 3-year-old boy presented with progressive behavioral disturbances with hypertronia and abnormal gait for the past 1 year. (A) Axial T2WI shows hyperintensity in the cerebellar white matter and dentate nuclei (white arrowhead); (B) extensive supratentorial white matter hyperintensities are noted, with frontal predominance and involvement of subcortical white matter. Capping is noted adjacent to the frontal horns bilaterally, hypointense on T2 (B) (white arrow), and hyperintense on T1WI (C). Bilateral striatal atrophy with altered signal intensity noted with associated dilatation of the lateral ventricles. (D and E) Axial T1 postcontrast reveals enhancement of the dentate nucleus and peridentate cerebellar white matter (white arrows) as well as the periventricular rim (white arrowheads)

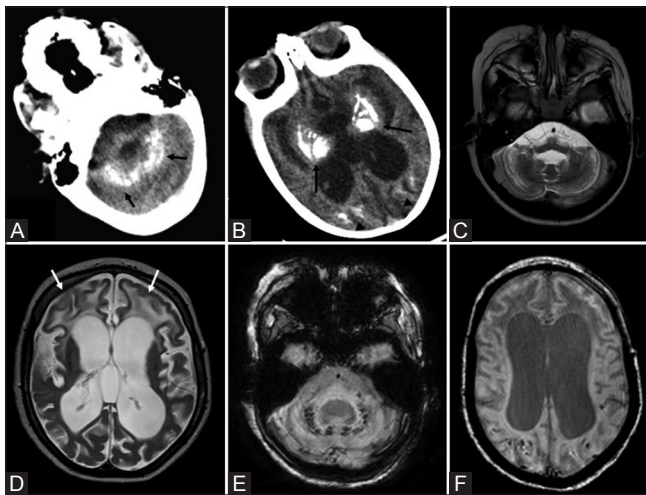


Figure 4 (A-F): Aicardi–Goutier syndrome – A 7-year-old boy presented with microcephaly, early onset feeding difficulties, and developmental delay. Axial CT sections of the brain show coarse calcifications in the dentate and cerebellar white matter (A) (black arrows), basal ganglia (black arrows), and subcortical white matter (black arrowheads) (B). (C and D) Axial T2WI reveals gross cerebellar and cerebral atrophy. There is extensive frontal predominant white matter hyperintensity (white arrows). (E and F) Axial SWI shows punctate calcifications of the dentate and subcortical white matter. CSF showed lymphocytosis and increased IFN- α . Serology was negative for TORCH infections

with profound hypodensity and swelling of the cerebellar hemispheres including dentate, dorsal part of the pons, midbrain, posterior limb of the internal capsule, the globus pallidus, and often the thalamus. These areas appear

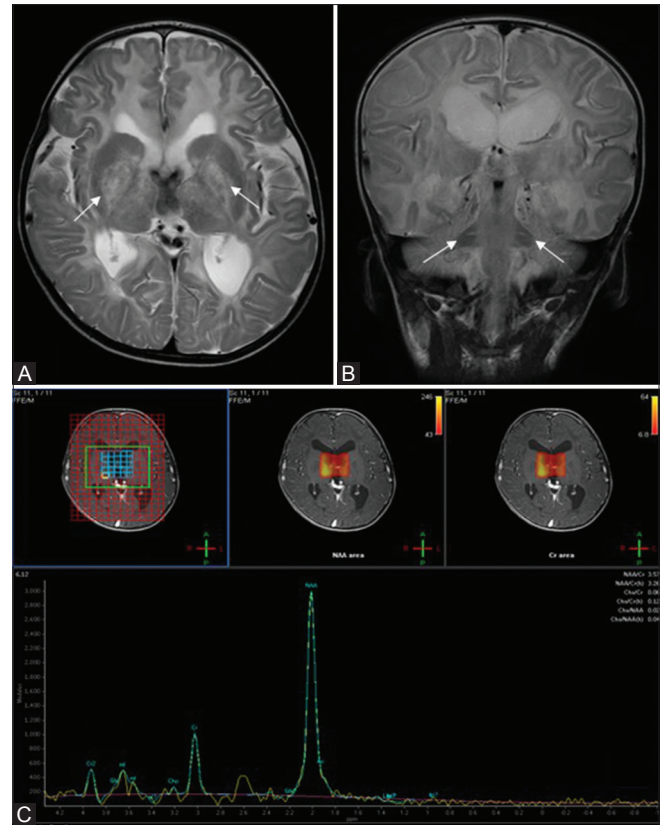


Figure 3 (A-C): Canavan's disease – An 8-month-old girl presented with hypotonia, cortical blindness, and macrocephaly since 3 months of age. (A) Axial T2WI shows extensive hyperintense signal changes in the supratentorial white matter with involvement of the subcortical U-fibres. Patchy signal change is also noted in the globi pallidi (white arrows) and anterolateral thalami bilaterally. (B) Coronal T2WI shows similar signal changes with involvement of the dentate hilus bilaterally (white arrows). (C) MRS at TE 135 ms from the basal ganglia shows large NAA peak at 2.02 ppm

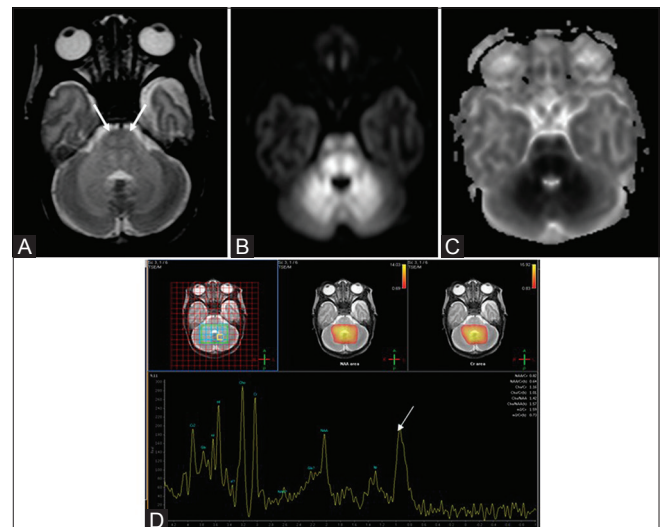


Figure 5 (A-D): Maple syrup urine disease – A 4-day-old infant presented with lethargy, poor feeding convulsions, bulging fontanelle, and irregular respiration. (A) Axial T2WI shows hyperintensity in the cerebellar white matter, dentate nuclei, pyramidal tracts (white arrows), and dorsal pons. DWI (B) and ADC (C) map shows diffusion restriction in the described areas. (D) MRS at TE 135 ms shows prominent amino acid peaks at 0.9 ppm (white arrow)

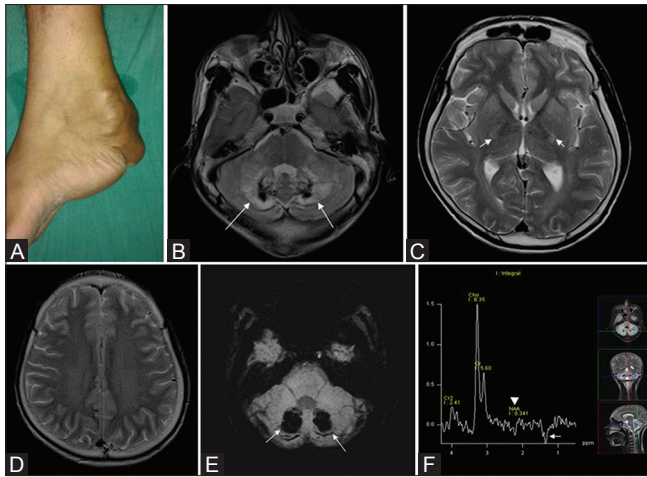


Figure 6 (A-F): Cerebro-tendinous xanthomatosis – A 23-year-old wheel-chair bound male with multiple subcutaneous swellings and mental retardation. (A) Clinical image of the right lower limb shows subcutaneous swelling – tendon xanthomas. (B) Axial T2WI reveals trilaminar appearance in the cerebellar hemisphere; hyperintensity in the core of the dentate nuclei; surrounding hypointensity suggestive of calcification and cerebellar white matter hyperintensity (*white arrows*). (C) and (D) images show subtle signal changes along the Corticospinal tracts (*white arrows*) and centrum semiovale. (E) SWI shows intense blooming of the dentate and adjacent white matter (*white arrows*) (F) MRS at TE 135 ms shows inverted lactate peak from the cerebellar white matter (*white arrow*) and decreased NAA peak (*white arrowhead*)

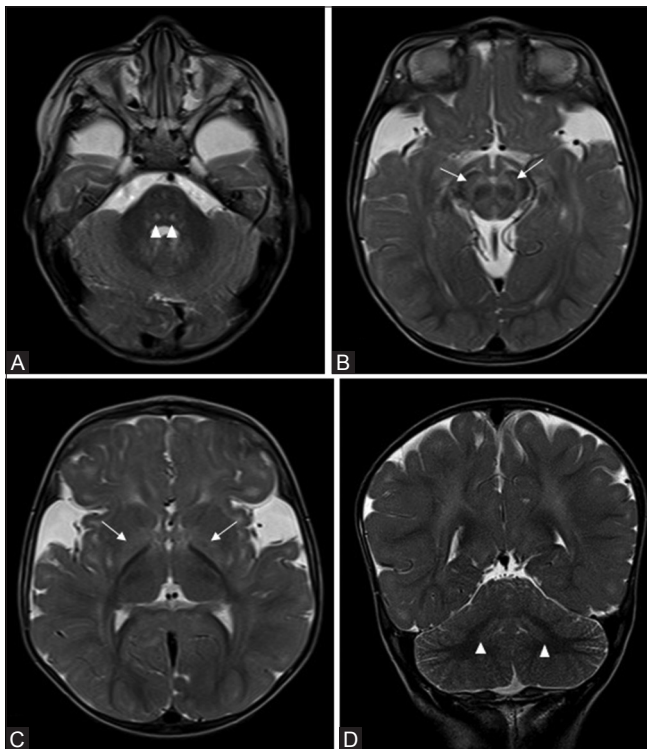


Figure 8 (A-D): Glutaric aciduria type-1 a 1½-year-old boy presented with developmental regression after an episode of febrile seizures at 9 months of age. Axial T2WI reveals hyperintense signal changes in the central tegmental tracts (A) (*white arrowheads*), brainstem (B) (*white arrows*), and globus pallidus (C) (*white arrows*), with wide open sylvian fissures. (D) Coronal T2WI shows hyperintensity in lobar white matter and dentate nuclei (*white arrowheads*)

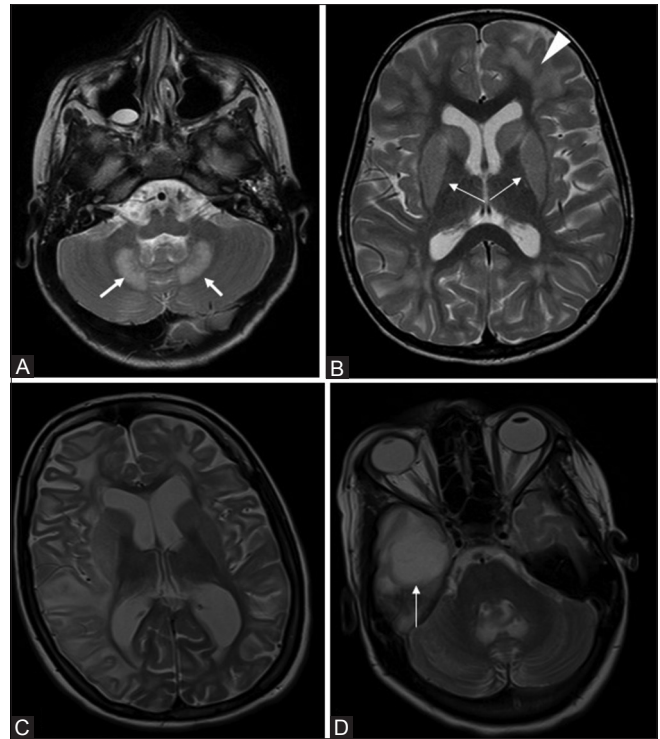


Figure 7 (A-D): L-2-hydroxyglutaric aciduria – Patient 1: A 4-year-old girl presented with ataxia, nystagmus, dysarthria, slow intellectual decline, and dystonia. (A) Axial T2WI shows hyperintensity in bilateral dentate nuclei and adjacent cerebellar white matter (*white arrow*). (B) Confluent signal changes in the supratentorial white matter with predominant subcortical involvement (*white arrowhead*). Bilateral symmetrical signal changes are also noted in the striatum (*white arrow*). Patient 2: A 9-year-old boy presented with a long-standing history of seizures, extrapyramidal symptoms, and ataxia. (C) Axial T2WI image shows signal changes similar to those of patient 1. (D) A cystic lesion in the right anterior temporal lobe is noted (*white arrow*). Postcontrast scan (not shown) did not reveal any enhancement. Postoperative histopathological examination showed a low-grade glioma

hyperintense in T2 and show diffusion restriction. MRS shows elevated branched chain amino acids and ketoacids at 0.9 ppm [Figure 5].

Cerebro-tendinous xanthomatosis is a rare autosomal recessive disorder of lipid metabolism, characterized by tendon xanthomas, early cataracts, mental deterioration, and spastic-ataxia. Involvement of spinal cord is also noted in some cases. CT may show dentate calcifications. MRI shows characteristic trilaminar appearance of the dentate, as shown in Figure 6. Hyperintense signal is also noted in supratentorial white matter, especially along the posterior limbs of internal capsules.

L-2 hydroxyglutaric aciduria has an autosomal recessive mode of inheritance. The age of presentation is relatively older than that of Canavan's disease. It is characterized by elevated levels of l-2-hydroxyglutarate in urine, CSF, and plasma. Imaging shows T2/FLAIR hyperintensity of the subcortical white matter, sparing the deep white

matter. Globus pallidus, caudate, and putamen are typically involved. Dentate may be involved. Diffuse gliomas have also been reported with the condition [Figure 7].^[6]

Glutaric aciduria type 1 is an autosomal recessive metabolic disorder caused due to the deficiency of glutaryl CoA dehydrogenase enzyme. Most cases present during infancy with acute encephalopathic illness along with seizures, hypotonia, and choreoathetosis precipitated by fever, immunization, or surgical procedure. MRI shows a large head size with wide open sylvian fissure due to failure of operculization, signal changes in the basal ganglia, and bilateral subdural collections. Dentate may be occasionally involved [Figure 8].

Mucopolysaccharidoses represent a group of inherited lysosomal storage disorders characterized by defective degradation of glycosaminoglycans. The clinical manifestations include short stature, skeletal deformities,

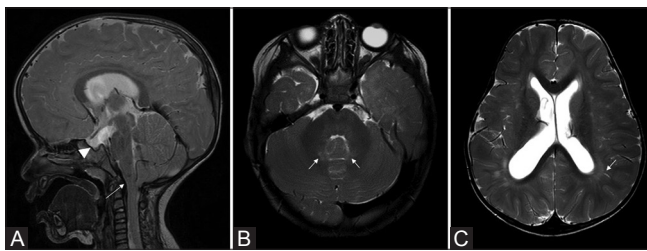


Figure 9 (A-C): Mucopolysaccharidosis – A 2½-year-old boy presented with facial dysmorphism, macrocephaly, and developmental delay. (A) T2W sagittal image shows craniofacial disproportion, J-shaped sella (*white arrowhead*) with crowding at the foramen magnum (*white arrow*). (B) and (C) T2W axial image shows T2 hyperintensity in dentate nuclei (*white arrows*). Posterior predominant prominent perivascular spaces in cerebral white matter are noted (C) (*white arrow*)

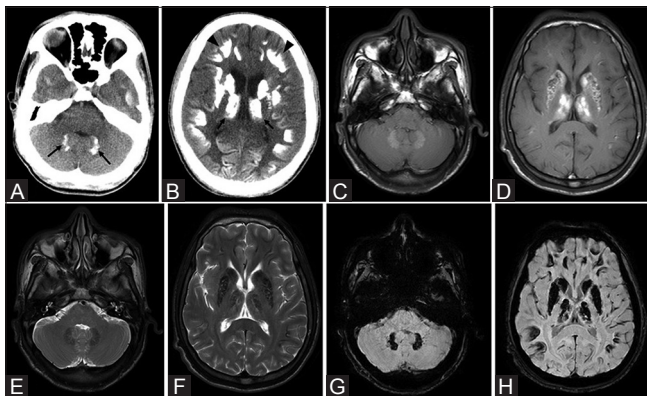


Figure 11 (A-H): Fahr disease – A 48-year-old male presented with tremors and slowness progressive in nature. Noncontrast CT brain shows extensive coarse calcifications of the dentate nuclei (A) (*black arrow*), thalami (*black arrow*), basal ganglia, and subcortical white matter (*black arrowheads*) (B). (C and D) Axial T1WI show patchy hyperintensity in these regions, T2WI shows hypointensity (E and F). (G and H) SWI shows blooming in these regions suggestive of calcification. Serum evaluation for other metabolic or systemic disorders was normal

hepatosplenomegaly, hernias, coarse facial features with cardiovascular, respiratory, and neurological abnormalities. MRI may show large head size, with J-shaped sella, prominent perivascular spaces, and crowding at Foramen magnum. Dentate may be involved [Figure 9].

Metronidazole toxicity is a known cause of abnormal T2 hyperintense signal change in dentate nuclei. This toxicity generally presents with dysarthria, ataxia, and visual blurring. Cumulative dose of 25–90 g administered over a period of 1–3 months is implicated.^[3] Symptomatic as well as imaging reversal is noted post drug withdrawal [Figure 10].

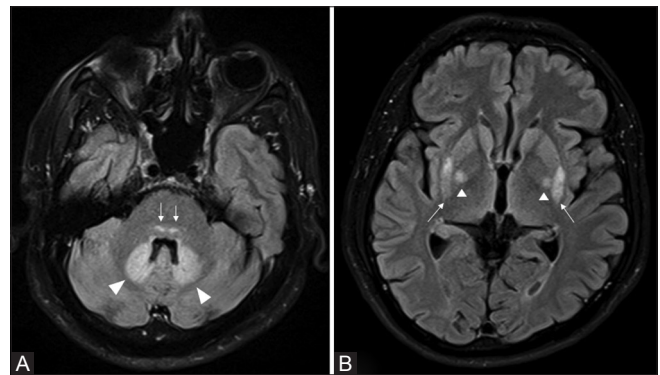


Figure 10 (A and B): Metronidazole toxicity – A 31-year-old man presented with acute onset ataxia and dysarthria. History revealed intake of metronidazole for 2 months. (A) Axial FLAIR images reveal bilateral symmetrical hyperintensity in the dentate nuclei (*white arrowhead*), central tegmental tracts (*white arrows*), dorsal pons, and (B) posterior putamina (*white arrows*) and globi pallidi (*white arrowheads*). There was no evidence of diffusion restriction or postcontrast enhancement (not shown)

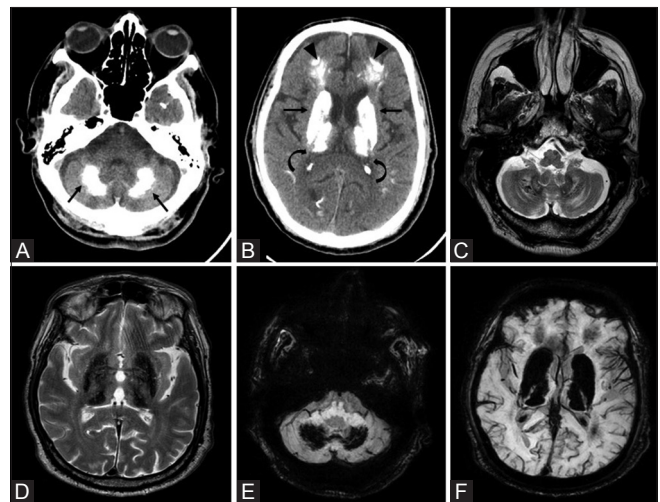


Figure 12 (A-F): Lead toxicity – A 40-year-old worker in pipe manufacturing industry for the past 20 years presented with extrapyramidal features. Axial CT images show calcification of dentate nuclei (A) (*black arrow*); basal ganglia (*black arrow*), thalami (*curved arrow*), and subcortical white matter (*black arrowhead*) (B). (C and D) T2W Axial MRI shows hypointensity in the dentate nuclei, thalami and basal ganglia, hyperintensity is noted in the cerebellar white matter. (E and F) SWI shows blooming in these regions. Serum evaluation for other metabolic or systemic disorders was normal

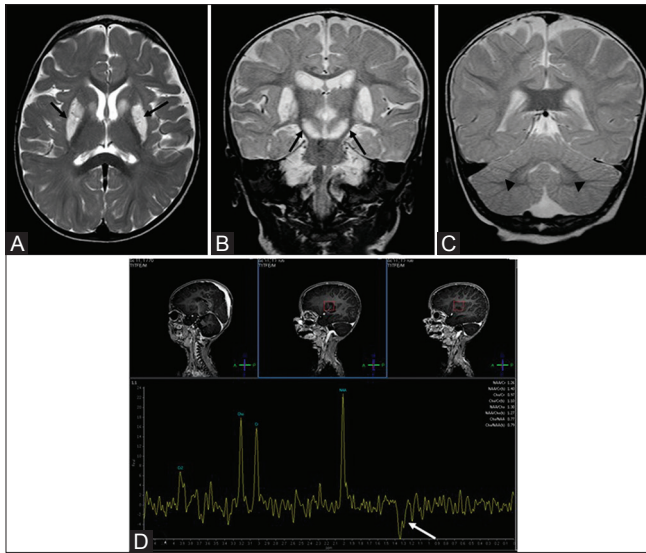


Figure 13 (A-D): Leigh disease with *SURF-1* mutation – A 1-year-old girl presented with regression of milestones along with feeding difficulties, following a febrile episode 4 months ago. (A) Axial T2WI reveals bilateral symmetrical hyperintense signal in the caudate, putamen (black arrows). (B and C) Coronal T2WI shows bilateral symmetrical hyperintense signal in substantia nigra (black arrows), subthalamic nuclei, and dentate nuclei (black arrowheads). Patchy areas of diffusion restriction and postcontrast enhancement were noted in these regions (not shown). (D) MRS at TE 135 ms shows inverted lactate peaks at 1.33 ppm (white arrows)

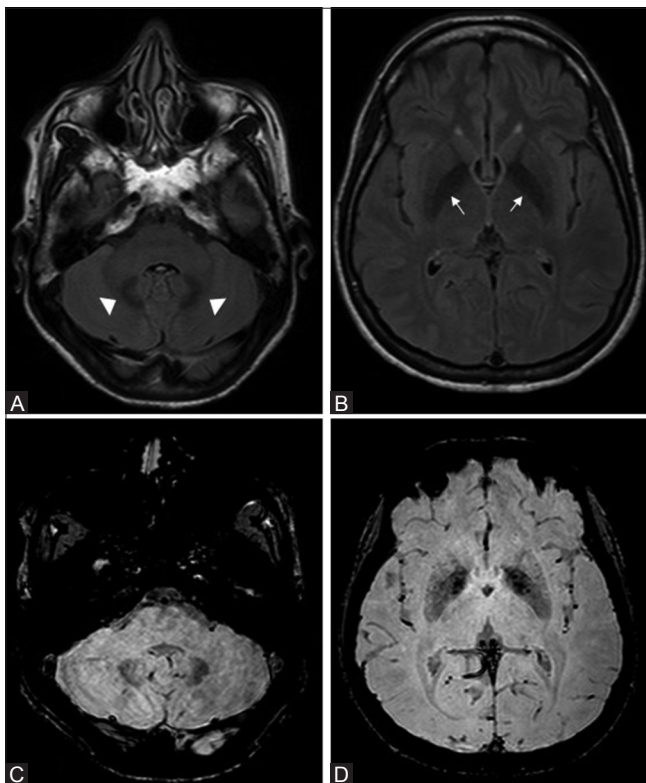


Figure 15 (A-D): Neuroferritinopathy – A 19-year-old female presented with extrapyramidal symptoms progressive for the last 2 years. Axial FLAIR images show hypointense signal in the dentate nuclei (A) (white arrowheads) and globus pallidus (B) (white arrows). These regions demonstrate blooming on GRE images (C) and (D)

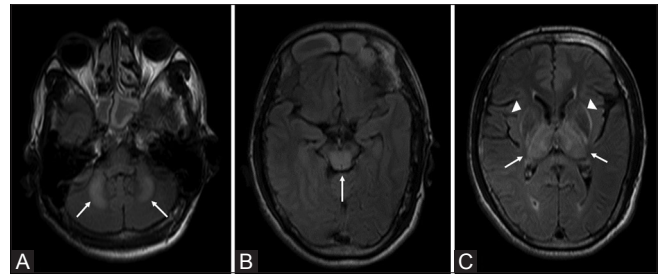


Figure 14 (A-C): Wilson's disease – A 14-year-old girl with KF ring and hepatomegaly. Axial FLAIR images of show bilateral symmetrical hyperintensity in the dentate nuclei and adjacent cerebellar white matter (A) (white arrows), dorsal midbrain (B) (white arrow), thalami (white arrows), and basal ganglia (C) (white arrowheads)

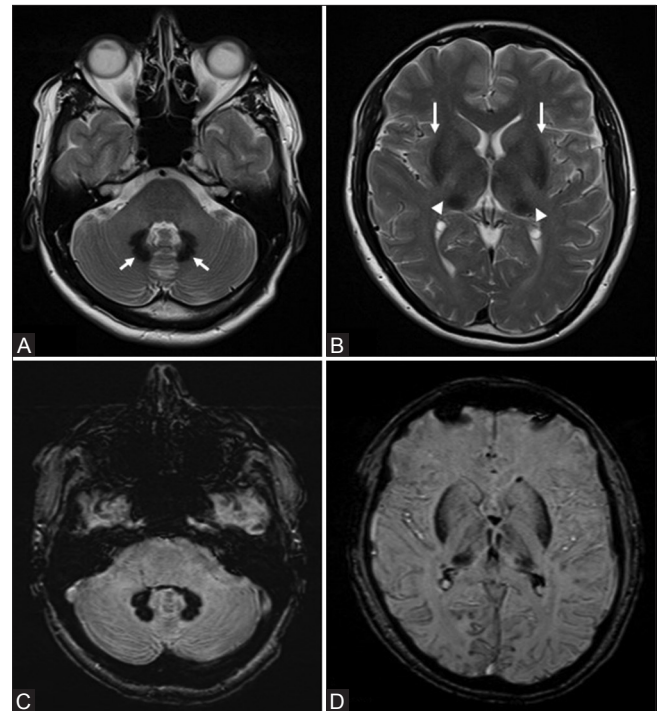


Figure 16 (A-D): Aceruloplasminemia – A 27-year-old male with tremors and intellectual impairment since 5 years. Axial T2WI images show bilateral symmetrical hypointensity in dentate nuclei (A) (white arrows), thalami (white arrowheads), and putamina (white arrows) (B). Intense blooming is noted in GRE images in these areas (C and D). No signal changes were noted in white matter

Isoniazid-associated cerebellitis has been described in patients on antitubercular treatment with coexistent chronic renal disease. It can present with bilateral dentate T2/FLAIR hyperintensity and diffusion restriction. Follow-up after withdrawal generally shows resolution of signal changes.^[7]

Fahr's syndrome is an autosomal dominant disorder, presents in 4th to 5th decade characterized by progressive neurologic dysfunction and neuropsychiatric manifestations. Biochemical abnormalities and somatic features suggestive of a metabolic disease or infectious, toxic, and traumatic causes should be excluded. Extensive calcifications can

be seen in the subcortical white matter, basal ganglia, and dentate, as shown in Figure 11.

Chronic lead poisoning is seen most commonly due to occupational exposure in workers involved in the manufacture of lead pipes and batteries. They can present with nonspecific neurologic manifestations such as dementia, diminished visual acuity, peripheral neuropathy, syncope, dizziness, nystagmus, easy fatigue, and back pain. It can be associated with extensive intracranial calcifications [Figure 12].^[8]

Leigh disease or subacute necrotizing encephalomyelopathy is a progressive neurodegenerative disorder caused by mitochondrial respiratory enzyme chain defects, characterized by developmental regression, and is often associated with febrile episodes and is caused by enzyme deficiencies of the respiratory chain complexes [Figure 13]. T2 hyperintensity is noted in the basal ganglia, brainstem, and dentate nuclei with diffusion restriction and postcontrast enhancement, which may be seen in acute stages. Involvement of brainstem and subthalamic nuclei has been described as an indicator of *SURF-1* mutations in cases of cytochrome oxidase deficiency.^[9]

Wilson's disease is an autosomal recessive disorder with defect in copper metabolism; it is characterized by abnormal accumulation of copper in various tissues, particularly in the liver and brain. Flapping tremors are classical findings in neurological examination along with Kaiser–Fleischer ring. MRI shows signal changes in basal ganglia, brainstem, and dentate, with occasional hyperintensity of cortex and subcortical white matter, especially frontal lobes [Figure 14].

Neurodegenerative

Neurodegeneration with brain iron accumulation (NBIA) is a group of progressive neurological disorders that present

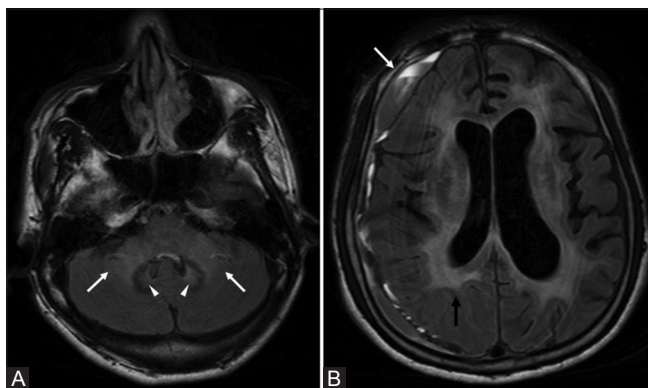


Figure 17 (A and B): Progressive multifocal leukoencephalopathy – A 40-year-old immunocompromised male presented with altered sensorium. Axial FLAIR images show bilateral asymmetrical hyperintense signal changes in the dentate nuclei (white arrowheads), middle cerebellar peduncles (A) (white arrows) and (B) supratentorial white matter with subcortical involvement in the left frontal lobe. Right-sided subdural hemorrhage was noted incidentally (white arrow)

with prominent extrapyramidal symptoms, intellectual impairment, and iron deposition in basal ganglia. Ten forms of NBIA have been described to date,^[10] of which neuroferritinopathy and aceruloplasminemia have been associated with iron deposition in dentate nuclei [Figures 15 and 16].^[11]

Inflammatory and infectious

Progressive multifocal leukoencephalopathy is a fulminating opportunistic infection of the brain caused by John Cunningham virus (JC virus) in a setting of immunocompromised status leading to myelin breakdown and oligodendrocyte destruction.^[5] Diffuse but bilateral asymmetrical signal changes are noted in the supra- and infratentorial white matter with involvement of subcortical areas [Figure 17]. Occasional postcontrast enhancement may be seen.

Langerhans's cell histiocytosis (LCH) presents with reactive clonal proliferation of Langerhans cells, which are bone marrow-derived cells of dendritic cell line with antigen presenting and processing properties. CNS imaging reveals craniofacial bones, skull base and paranasal sinus invasion, involvement of meninges and hypothalamo-pituitary axis is noted.^[12] Patchy lesions with postcontrast enhancement may be seen; involvement of dentate is common [Figure 18].

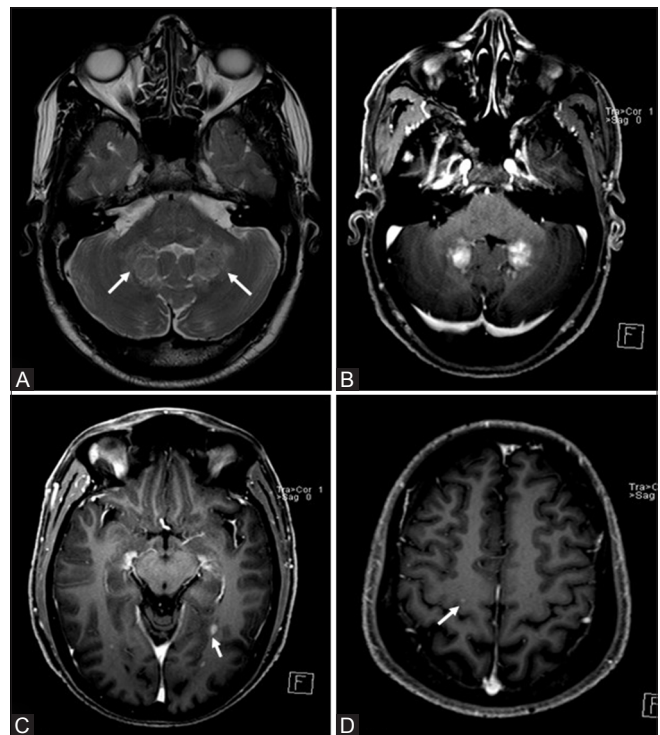


Figure 18 (A-D): Langerhans cell histiocytosis – A 30-year-old man presented with ataxia for 4 months and hepatosplenomegaly. (A) Axial T2WI shows bilateral symmetrical patchy hyperintense signal change in the dentate nuclei (white arrows), which shows intense postcontrast enhancement (B). (C and D) Multiple other enhancing punctate foci are noted in the subcortical white matter (white arrows). Histopathology from biopsy from temporal lobe showed findings consistent with LCH

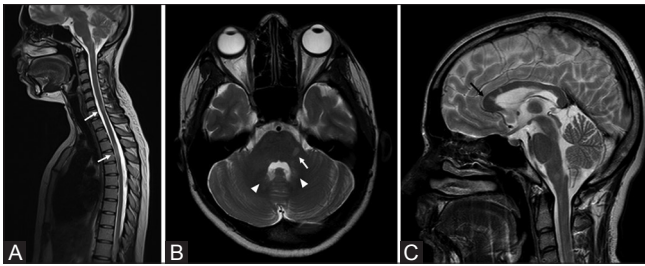


Figure 19 (A-C): Multiple sclerosis – A 16-year-old girl presented with relapsing remitting neurological illness since the last 2 years. (A) T2W sagittal image of the spine shows patchy short segment hyperintensities in the cervicodorsal cord (*white arrows*). Similar signal changes are noted in bilateral dentate nuclei (*white arrowheads*), left middle cerebellar peduncle (B) (*white arrow*), medulla, and corpus callosum (C) (*black arrow*)

Erdheim–Chester disease is a non-Langerhans cell form of histiocytosis characterized by xanthomatous infiltration of tissues by foamy histiocytes. Multiple organ infiltration is also noted in this entity, as in LCH. Diametaphyseal osteosclerotic lesion of long bones showing increased uptake in Tc 99m bone scintigraphy form radiological diagnostic criteria. Dentate involvement has been described in this entity.^[13]

Multiple sclerosis (MS) is the most common chronic inflammatory demyelinating disease affecting young adults mostly leading to severe and irreversible clinical disability. The demyelinating plaques can be noted in the supratentorial (periventricular and juxtacortical) as well as infratentorial parenchyma and spinal cord. Dentate involvement has been described as T1 hyperintensity in unenhanced images, which are more commonly associated with the secondarily progressive subtype.^[14] T2 hypointensity in dentate has also been correlated with ambulatory impairment in MS.^[15] [Figure 19].

Miscellaneous

Gadolinium-based contrast agent (GBCA) exposure – Of the other causes of dentate involvement, gadolinium deposition in dentate nuclei is important. It can be observed in patients who require repeated imaging with GBCAs. The patients generally have preserved renal function. Deposition is also seen in the globus pallidus and is most commonly associated with use of gadodiamide (nonionic linear chelate). It is now considered that the T1 hyperintensity in the dentate nuclei of MS patients may be attributed to the repeated exposure to GBCAs and gadolinium deposition given the repeated MRI done in these patients.^[16] Recent studies performed on autopsy specimens proved that T1 shortening results from gadolinium retention in neuronal tissues of the globus pallidus, thalamus, dentate nucleus, and pons [Figure 20].

Conclusion

We have presented the dentate involvement in many commonly encountered conditions in neuroradiology

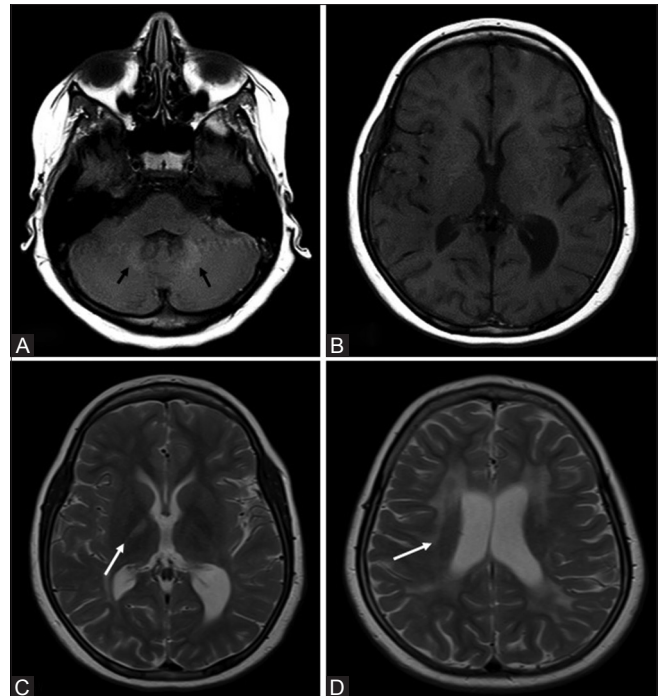


Figure 20 (A-D): Gadolinium-based contrast agent deposition – A 15-year-old girl had relapsing remitting neurological illness and had undergone 11 MRIs in the last 4 years. (A and B) Axial T1WI shows hyperintensity in the dentate nuclei in the recent MRI (*black arrow*); no obvious signal change was noted in globus pallidus. Axial T2WI reveals signal change in the right posterior limb of internal capsule (C) (*white arrow*) and periventricular white matter (*white arrow*)(D)

practice. Awareness of the conditions and imaging with CT and MRI individually or in conjunction with each other leads to the most plausible diagnosis in almost all instances.

Financial support and sponsorship

Nil.

Conflicts of interest

There are no conflicts of interest.

References

- Blaser S, Steinlin M, Al-Maawali A, Yoon G. The Pediatric Cerebellum in Inherited Neurodegenerative Disorders. *Neuroimaging Clin N Am* 2016;26:373-416.
- McErlean A, Abdalla K, Donoghue V, Ryan S. The dentate nucleus in children: Normal development and patterns of disease. *Pediatr Radiol* 2010;40:326-39.
- Khadilkar S, Jaggi S, Patel B, Yadav R, Hanagandi P, Faria do Amaral L. A practical approach to diseases affecting dentate nuclei. *Clin Radiol* 2016;71:107-19.
- Sedghizadeh P, Nguyen M, Enciso R. Intracranial physiological calcifications evaluated with cone beam CT. *Dentomaxillofac Radiol* 2012;41:675-8.
- Knaap M, Valk J, Barkhof F. *Magnetic Resonance of Myelination and Myelin Disorders*. Berlin [etc.]: Springer; 2005.
- Patay Z, Mills J, Lobel U, Lambert A, Sablauer A, Ellison D. Cerebral Neoplasms in L-2 Hydroxyglutaric Aciduria: 3 New Cases and Meta-Analysis of Literature Data. *Am J Neuroradiol*

- 2012;33:940-3.
7. Peter P, John M. Isoniazid-induced cerebellitis: A disguised presentation. *Singapore Med J* 2014;55.
 8. Reyes P, Gonzalez C, Zalewska M, Besarab A. Intracranial calcification in adults with chronic lead exposure. *Am J Roentgenol* 1986;146:267-70.
 9. Farina L, Chiapparini L, Uziel G, Bugiani M, Zeviani M, Savoiaro M. MR Findings in Leigh Syndrome with COX Deficiency and SURF-1 Mutations. *Am J Neuroradiol* 2002;23:1095-100.
 10. Hogarth P. Neurodegeneration with Brain Iron Accumulation: Diagnosis and Management. *J Mov Disord* 2015;8:1-13.
 11. Kruer M, Boddaert N. Neurodegeneration With Brain Iron Accumulation: A Diagnostic Algorithm. *Semin Pediatr Neurol* 2012;19:67-74.
 12. Prayer D, Grois N, Prosch H, Gadner H, J. Barkovich A. MR Imaging Presentation of Intracranial Disease Associated with Langerhans Cell Histiocytosis. *Am J Neuroradiol* 2004;25:880-91.
 13. NaS, Lee K, Kim J, Kim Y. A Case of Cerebral Erdheim-Chester Disease With Progressive Cerebellar Syndrome. *J Clin Neurol* 2008;4:45.
 14. Roccatagliata L, Vuolo L, Bonzano L, Pichiecchio A, Mancardi G. Multiple Sclerosis: Hyperintense Dentate Nucleus on Unenhanced T1-weighted MR Images Is Associated with the Secondary Progressive Subtype. *Radiology* 2009;251:503-10.
 15. Tjoa C, Benedict R, Weinstock-Guttman B, Fabiano A, Bakshi R. MRI T2 hypointensity of the dentate nucleus is related to ambulatory impairment in multiple sclerosis. *J Neurol Sci* 2005;234:17-24.
 16. McDonald R, McDonald J, Kallmes D, Jentoft M, Murray D, Thielen K, *et al.* Intracranial Gadolinium Deposition after Contrast-enhanced MR Imaging. *Radiology* 2015;275:772-82.